

The weak $\Delta S = 1$ ΛN interaction with effective field theory

Axel Pérez-Obiol*

*Departament d'Estructura i Constituents de la Matèria,
Institut de Ciències del Cosmos (ICC),
Universitat de Barcelona, Martí i Franquès 1, E-08028, Spain
E-mail: axel@ecm.ub.es*

Assumpta Parreño

*Departament d'Estructura i Constituents de la Matèria,
Institut de Ciències del Cosmos (ICC),
Universitat de Barcelona, Martí i Franquès 1, E-08028, Spain
E-mail: assum@ecm.ub.es*

Bruno Juliá-Díaz

*ICFO-Institut de Ciències Fotòniques, Parc Mediterrani de la Tecnologia, E-08860 Castelldefels
(Barcelona), Spain
Departament d'Estructura i Constituents de la Matèria,
Institut de Ciències del Cosmos (ICC),
Universitat de Barcelona, Martí i Franquès 1, E-08028, Spain
E-mail: bruno.julia@icfo.es*

David R. Entem

*Grupo de Física Nuclear e IUFFyM,
Universidad de Salamanca, E-37008 Salamanca, Spain
E-mail: entem@usal.es*

The relation between the low energy constants appearing in the effective field theory (EFT) description of the $\Lambda N \rightarrow NN$ transition potential and the parameters of the one-meson-exchange model previously developed is obtained. We extract the relative importance of the different exchange mechanisms included in the meson picture by means of a comparison to the corresponding operational structures appearing in the EFT approach. Constraints on weak baryon-baryon-meson couplings for a possible scalar exchange are also discussed. This work is based on the lowest order EFT approach of Ref. [1]. Higher order contributions are sketched.

*Sixth International Conference on Quarks and Nuclear Physics
April 16-20, 2012
Ecole Polytechnique, Palaiseau, Paris*

*Speaker.

1. The ΛN interaction and the One Meson Exchange model

The Λ hyperon decays in free space through the nonleptonic weak decay modes $\Lambda \rightarrow n\pi^0$ and $\Lambda \rightarrow p\pi^-$, with an approximate ratio of 36:64. This mechanism is highly suppressed in the nuclear medium, since the momentum of the nucleon in the final state is not large enough to access unoccupied states above the Fermi energy level. However, hypernuclear systems decay, precisely due to the presence of surrounding nucleons, by means of single-, $\Gamma_{1N} = \Lambda N \rightarrow NN$, and multi-nucleon induced decay mechanisms. The contribution to the decay rate from these mechanisms becomes more important for heavier hypernuclei (which have larger Fermi energy levels). It is through hypernuclear decay observables that we study the $\Lambda N \rightarrow NN$ interaction.

Traditionally, and in analogy with the strong NN interaction, the one-nucleon induced decay mode, $\Lambda N \rightarrow NN$, has been described by a one-boson-exchange model, in which ground states of the pseudoscalar and vector meson octets are exchanged [2]. Heavier mesons account for shorter distances, and yet higher energy physics is parametrized through explicit cut-offs of ≈ 1 GeV. The momentum space transition potential is given by the nonrelativistic limit of the appropriate Feynman amplitude depicted in Figs. 1(a) and 1(b). The six potentials, as well as the necessary baryon-baryon-meson Hamiltonians, are explicitly given in [1].

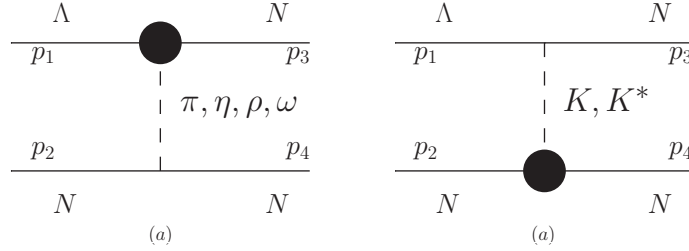


Figure 1: Non-strange (a) and strange (b) meson-exchange contributions to the $\Lambda N \rightarrow NN$ weak transition potential. A weak insertion is indicated by a solid circle.

2. Effective Field Theory

In order to study the $\Lambda N \rightarrow NN$ interaction in a less model dependent way, we build an effective field theory (EFT). In contrast to the one meson exchange (OME) model, this approach provides a systematic way of handling nonperturbative strong interaction physics. With this technique, the baryon-baryon interaction is separated into long- and short-distance components. Below a certain cut-off energy, an EFT describes the interaction involving the degrees of freedom appearing explicitly in this energy domain. In the nucleon-nucleon sector, these degrees of freedom are usually the nucleons and the pions, but when higher energies are involved, as in our case, heavier mesons and baryons must be included. The short distance dynamics are not accounted for by heavier mesons, as in the OME models, but by a series of contact terms that respect chiral symmetry, Lorentz invariance and the applicable discrete symmetries. These local interactions are organized as an increasing number of derivatives, so that each term corresponds to a given power of a small parameter in the theory, which in a baryon-baryon interaction is usually the ratio between a typical momentum and a baryon mass. In our case, the parameter is $\frac{\vec{q}}{M_N}$, where \vec{q} is the transferred mo-

momentum and M_N the nucleon mass. The local operators are accompanied by a series of low energy constants (LECs) that must be fitted to reproduce the experimental data (on hypernuclear decay).

The EFT for the non-leptonic weak $|\Delta S| = 1$ ΛN interaction was first formulated in Refs. [3, 4]. The authors in [3] constructed the effective theory by adding to the long-ranged one-pion-exchange mechanism (OPE) a four-fermion contact interaction, coming from Lorentz four-vector currents. Later, in Ref. [4], the K -exchange mechanism (OKE) was added to the intermediate range of the interaction, as well as additional operational structures to the short range part of the transition potential, as depicted in Fig. 2. The present work represents an update of the one performed in Ref. [4].

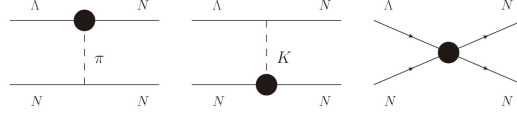


Figure 2: LO contributions to the potential: the OPE and OKE and a local term with no derivatives.

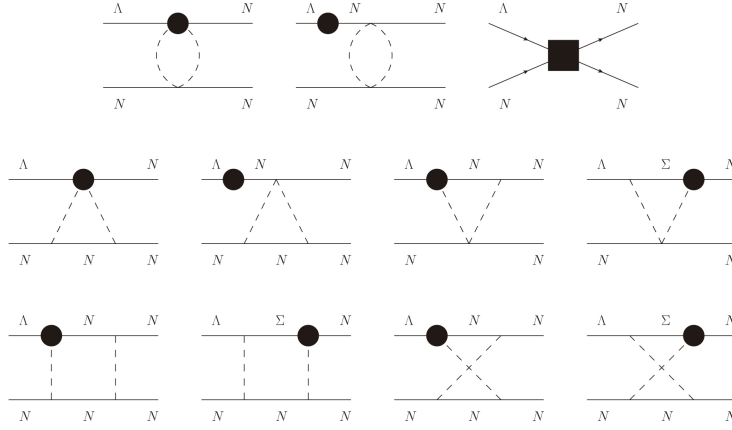


Figure 3: NLO contributions to the potential: 2π exchanges as well as local terms containing one derivative.

At next to leading order (NLO) one has to consider the contribution coming from the diagrams in Fig. 3 [5]. In particular, the calculation of diagrams containing an intermediate sigma baryon requires the knowledge of the strong $\Lambda\Sigma\pi$ vertex, obtained from the $SU(3)$ strong chiral Lagrangian,

$$\mathcal{L}_{\Lambda\Sigma\pi}^S = -\frac{D_s}{\sqrt{3}} \bar{\Psi}_\Lambda \gamma^\mu \gamma_5 \Psi_\Sigma \cdot \partial_\mu \vec{\pi}, \quad (2.1)$$

as well as the weak $\Sigma N\pi$ vertex, for which we take the following phenomenological Lagrangian

$$\mathcal{L}_{\Sigma N\pi}^W = -iG_F m_\pi^2 \bar{\Psi}_N \left[(A_{\Sigma\frac{1}{2}} + B_{\Sigma\frac{1}{2}} \gamma^5) \vec{\tau} \cdot \vec{\pi} \Psi_{\Sigma\frac{1}{2}} + (A_{\Sigma\frac{3}{2}} + B_{\Sigma\frac{3}{2}} \gamma^5) \vec{T} \cdot \vec{\pi} \Psi_{\Sigma\frac{3}{2}} \right], \quad (2.2)$$

where the parameters $A_{\Sigma\frac{1}{2}}$, $A_{\Sigma\frac{3}{2}}$, $B_{\Sigma\frac{1}{2}}$ and $B_{\Sigma\frac{3}{2}}$ are obtained from a fit to the non-leptonic decay of the Σ [6]. The weak $\Lambda N\pi\pi$ vertex, which is also needed at this order, can be obtained by expanding the weak $SU(3)$ chiral Lagrangian,

$$\mathcal{L} = G_F m_\pi^2 \frac{h_{\Lambda N}}{f_\pi^2} \bar{\Psi}_N \Psi_\Lambda \vec{\pi}^2. \quad (2.3)$$

Notice that, in contrast to the $\Lambda N\pi$ vertex, the coupling appearing in the $\Lambda N\pi\pi$ Lagrangian is not fitted to experimental data and introduces more uncertainty to the theory through the parameter $h_{\Lambda N}$.

partial wave	operator	size	I
$^1S_0 \rightarrow ^1S_0$	$\hat{1}, \vec{\sigma}_1 \vec{\sigma}_2$	1	1
$^1S_0 \rightarrow ^3P_0$	$(\vec{\sigma}_1 - \vec{\sigma}_2)\vec{q}, (\vec{\sigma}_1 \times \vec{\sigma}_2)\vec{q}$	q/M_N	1
$^3S_1 \rightarrow ^3S_1$	$\hat{1}, \vec{\sigma}_1 \vec{\sigma}_2$	1	0
$^3S_1 \rightarrow ^1P_1$	$(\vec{\sigma}_1 - \vec{\sigma}_2)\vec{q}, (\vec{\sigma}_1 \times \vec{\sigma}_2)\vec{q}$	q/M_N	0
$^3S_1 \rightarrow ^3P_1$	$(\vec{\sigma}_1 + \vec{\sigma}_2)\vec{q}$	q/M_N	1
$^3S_1 \rightarrow ^3D_1$	$(\vec{\sigma}_1 \times \vec{q})(\vec{\sigma}_2 \times \vec{q})$	q^2/M_N^2	0

Table 1: $\Lambda N \rightarrow NN$ transitions for an initial ΛN relative S -wave state.

For the contact interactions we rely directly on the terms which enter at each order given the symmetries fulfilled by the weak $|\Delta S| = 1$ transition. All possible transitions are shown in Table 1 for an initial S -wave $\Lambda - N$ state, where, the model independent leading order operators in momentum space are listed. Organizing all these contributions in increasing size operators, we obtain the most general Lorentz invariant potential, for the four-fermion (4P) interaction in momentum space up to $\mathcal{O}(q^2/M^2)$ order (in units of $G_F = 1.166 \times 10^{-11} \text{ MeV}^{-2}$):

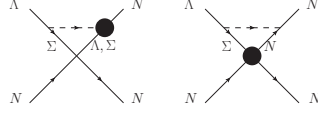
$$\begin{aligned}
V_{4P}(\vec{q}) = & C_0^0 + C_0^1 \vec{\sigma}_1 \vec{\sigma}_2 \\
& + C_1^0 \frac{\vec{\sigma}_1 \vec{q}}{2M} + C_1^1 \frac{\vec{\sigma}_2 \vec{q}}{2M} + iC_1^2 \frac{(\vec{\sigma}_1 \times \vec{\sigma}_2) \vec{q}}{2M} \\
& + C_2^0 \frac{\vec{\sigma}_1 \vec{q} \vec{\sigma}_2 \vec{q}}{4MM} + C_2^1 \frac{\vec{\sigma}_1 \vec{\sigma}_2 \vec{q}^2}{4MM} + C_2^2 \frac{\vec{q}^2}{4MM}.
\end{aligned} \tag{2.4}$$

In order to distinguish which contributions enter at a certain order in the perturbative potential we make use of Weinberg power counting [7]. In Figs. 2 and 3 we show which topologies enter at leading and next to leading order in our EFT. All these diagrams are calculated in the heavy baryon formalism [8]. The calculations are analogous to the ones done in the strong NN interaction except for a couple of difficulties characteristic to the $\Lambda N \rightarrow NN$ transition. First, the term $\bar{\Psi}_N(B_\pi \gamma_5) \vec{\tau} \vec{\phi}^\pi \Psi_\Lambda$ appearing in the weak $\Lambda N\pi$ Hamiltonian enters at second order in the heavy baryon expansion, and a priori one should neglect it in front of $\bar{\Psi}_N A_\pi \vec{\tau} \vec{\phi}^\pi \Psi_\Lambda$. Nevertheless, the constants A_π and B_π , adjusted to reproduce the free-space Λ decay, fulfill the relation $|B_\pi| \simeq 7|A_\pi|$, compensating thus the difference in heavy baryon orders. Second, in the loop integrals appearing at NLO, specifically in the denominators coming from the baryon propagators, appear quantities of the type $M_\Lambda - M_N$ and $M_\Sigma - M_N$. When the initial and final particles are the same, these transferred energies don't appear and the integrals become more simple.

Notice that the 1π corrections to the LO contact interactions, as for example the ones in Fig. 4, also enter at NLO. These diagrams only shift the coefficients of the LO contact terms with m_π , $M_\Lambda - M_N$ and $M_\Sigma - M_N$ dependent functions.

3. LO fit and comparison to the OME

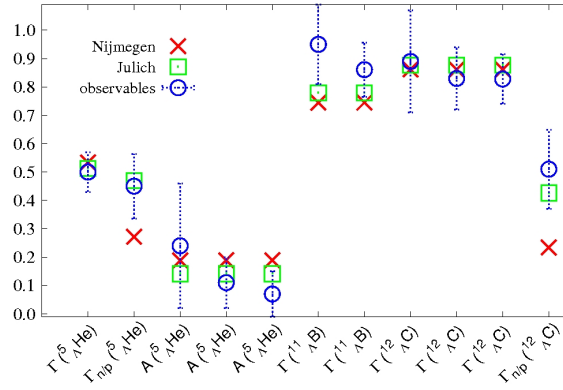
The potential at LO is written as the sum of the OPE and OKE potentials and the LO part of


Figure 4: Two corrections to LO contact interactions

the 4-point interaction potential.

$$V_{LO}(\vec{q}) = V_{\pi}(\vec{q}) + V_K(\vec{q}) + V_{4p}(\vec{q}; C_0^0, C_0^1) \quad (3.1)$$

There are two free parameters, C_0^0 and C_0^1 , that need to be fitted to the hypernuclear decay data. We have three independent observables: the total nonmesonic decay rate, $\Gamma(\Lambda N \rightarrow NN)$; the partial decay rate, $\frac{\Gamma(\Lambda n \rightarrow mn)}{\Gamma(\Lambda p \rightarrow np)}$; and the asymmetry, $A = \frac{N^+(p) - N^-(p)}{N^+(p) + N^-(p)}$, with $N^+(p)$ ($N^-(p)$) the number of protons going up (down) with respect to the hypernuclear polarization axis, and which is related to the interference between parity violating (PV) and parity conserving (PC) amplitudes of the weak transition. A LO fit to these observables for three different hypernuclei, ${}^{\Lambda}_5\text{He}$, ${}^{\Lambda}_{11}\text{B}$ and ${}^{\Lambda}_{12}\text{C}$, has been performed. The results are shown in Fig. 5 together with the experimental values. Our calculation receives the input of strong interaction models through the baryon-baryon-kaon coupling constants, form factors and the derivation of the baryon-baryon wave functions within the T-matrix formalism [2]. In Fig. 5 we show our results for two different strong interaction models, Jülich [9] and Nijmegen [10]. It can be seen that the available experimental database for the hypernuclear decay is described with good accuracy by this LO EFT potential.


Figure 5: Hypernuclear decay observables (total and partial decay rates and asymmetry for ${}^{\Lambda}_5\text{He}$, ${}^{\Lambda}_{11}\text{B}$ and ${}^{\Lambda}_{12}\text{C}$), and their fitted values. The total decay rates are in units of the Λ decay rate in free space ($\Gamma_{\Lambda} = 3.8 \times 10^9 \text{s}^{-1}$). All the quantities are adimensional.

In order to understand the dynamical origin of higher energy physics encapsulated in the contact interactions, we have related the LECs appearing in the LO EFT potential with the heavy meson parameters appearing in the OME potentials. This procedure is called resonance saturation and has been previously applied to the NN interaction by other authors [11].

Since the OPE and OKE appear explicitly in both potentials we only need to compare the operator structures appearing in the EFT local terms with the ones appearing in the heavy meson potentials (η , ω , ρ and K^*). In the EFT these are naturally organized in increasing powers of momentum. In contrast, the OME potentials must be expanded in powers of \vec{q} , so each operator structure comes accompanied by a definite power of transferred momentum \vec{q} .

	Nijmegen		Jülich	
	OME expansion	LO PC calculation	OME expansion	LO PC calculation
C_0^0	1.07 ± 0.88	(4.01 ± 0.23)	-1.7 ± 2.6	(4.03 ± 0.50)
C_0^1	0.02 ± 0.36	(0.02 ± 0.33)	0.12 ± 0.37	(-0.30 ± 0.28)

Table 2: Values for the LECs obtained from the two sources: OME expansion and LO (PC) EFT calculation, using the Nijmegen and Jülich strong interaction models. All the quantities are in units of $G_F = 1.166 \times 10^{-11} \text{ MeV}^{-2}$.

In Table 2 we compare the numerical values for the LO LECs obtained with the EFT fit and with the expansion of the OME potentials. The largest discrepancy appears in the C_0^0 LEC. This finding partly motivated us to consider explicitly a scalar isoscalar operator in the OME picture, in the form of a sigma meson. This inclusion produces an additional contribution to the C_0^0 OME LEC, $-\frac{m_\sigma^2}{m_\pi^2} A_\sigma g_{NN\sigma}$, where $g_{NN\sigma}$ is the sigma coupling, m_σ and m_π the sigma and pion masses and A_σ parametrizes the PC part of the weak $\Lambda N\sigma$ vertex. This procedure can be used to set bounds on the (unknown) values for A_σ . For example, taking the values of $m_\sigma = 550 \text{ MeV}$ and $g_{NN\sigma} = 8.8$ from Ref. [12], and working within the Nijmegen strong potential model, $3.3 \leq A_\sigma \leq 7.3$, as derived in Ref. [1].

This work has been partially supported by the contracts FPA2010-21750-C02-02 and FIS2008-01661 from MICINN (Spain) and by the Generalitat de Catalunya contract 2009SGR-1289. We acknowledge the support of the European Community-Research Infrastructure Integrating Activity ‘‘Study of Strongly Interacting Matter’’ (HadronPhysics2, Grant Agreement n. 227431) under the Seventh Framework Programme of EU. A. P-O. acknowledges the APIF PhD scholarship program of the University of Barcelona.

References

- [1] A. Pérez-Obiol, A. Parreño and B. Juliá-Díaz, Phys. Rev. **C84**, 024606 (2011).
- [2] A. Parreño, A. Ramos, and C. Bennhold, Phys. Rev. **C56**, 339 (1997).
- [3] Jung-Hwan Jun, Phys. Rev. **C63**, 044012 (2001).
- [4] A. Parreño, C. Bennhold, and B.R. Holstein, Phys. Rev. **C70**, 051601 (2004); A. Parreño, C. Bennhold, and B.R. Holstein, Nucl. Phys. **A754**, 127c (2005).
- [5] A. Pérez-Obiol, D.R. Entem, B. Juliá-Díaz and A. Parreño, work in progress.
- [6] C. Chumillas, New Developments in the Weak Decay of Hypernuclei, Ph.D. Thesis (2011)
- [7] S. Weinberg, Phys. Lett. **B251**, 288 (1990); S. Weinberg, Nucl. Phys. **B363**, 3 (1991).
- [8] E. Jenkins and A. Manohar, Phys. Lett. **B255**, 558-562 (1991).
- [9] B. Holzenkamp, K. Holinde, and J. Speth, Nucl. Phys. **A500**, 485 (1989).
- [10] V.G.J. Stoks and Th.A. Rijken, Phys. Rev. **C59**, 3009 (1999); Th.A. Rijken, V.G.J. Stoks, and Y. Yamamoto, Phys. Rev. **C59**, 21-40 (1999).
- [11] E. Epelbaum, U. Meissner, W. Glöckle, and C. Elster, Phys. Rev. **C65**, 044001 (2002).
- [12] R. Machleidt, Adv. Nucl. Phys. **19**, 189 (1989).